European Journal of Operational Research 267 (2018) 304–314

Contents lists available at ScienceDirect

European Journal of Operational Research

journal homepage: www.elsevier.com/locate/ejor

Innovative Applications of O.R.

A portfolio model for siting offshore wind farms with economic and environmental objectives

Alexana Cranmer[a,*], Erin Baker[b], Juuso Liesiö[c], Ahti Salo[d]

[a] Marston 120B, Department of Mechanical and Industrial Engineering, University of Massachusetts, 160 Governors Drive, Amherst, MA 01003, United States
[b] Marston 120C, Department of Mechanical and Industrial Engineering, University of Massachusetts, 160 Governors Drive, Amherst, MA 01003, United States
[c] Department of Information and Service Economy, Aalto University School of Business, P.O. Box 21220, 00076 Aalto, Finland
[d] Systems Analysis Laboratory, Department of Mathematics and Systems Analysis, Aalto University School of Science, P.O. Box 11100, 00076 Aalto, Finland

ARTICLE INFO

Article history:
Received 23 January 2017
Accepted 10 November 2017
Available online 21 November 2017

Keywords:
OR in energy
Decision analysis
Integer programming
Networks
OR in environment and climate change

ABSTRACT

Siting offshore wind farms is a complex problem due to the wake interactions between wind farms. We develop a profit maximizing portfolio model based on underlying network models to track the wake effects through a series of wind farms. Our portfolio model optimizes the siting of wind farms considering multiple wind directions and wind speeds and performs better than simple decision heuristics. Excluding sites from the portfolio has nonlinear impacts on the profitability of the portfolio of sites in that areas excluded from consideration have greater impacts on profit if they are grouped together or aligned parallel to the prevailing wind direction. The model can be readily adapted to include additional cost factors.

1. Introduction

Generating electricity from offshore wind farms can help coastal regions meet growing electricity demands from renewable sources. There are many demands, however, on the offshore space from recreational, commercial, and conservation uses. This paper builds an optimization framework to address two challenges present in planning for siting offshore wind farms: 1) how to plan for a potentially large number of offshore wind farms in the presence of wake interactions at the wind farm level, and 2) how to account for the costs of excluding sites from the choice set for development due to competing demands.

Existing uses can preclude a significant portion of the wind resource from wind farm development (Sheridan, Baker, Pearre, Firestone, & Kempton, 2012). The U.S. National Renewable Energy Lab (NREL) set a target of 86 gigawatts of offshore wind in the U.S. in their Wind Vision Study (U.S. Department of Energy, 2014). Depending on the density of wind turbines, meeting this goal will require developing about 10% of the currently feasible Federal offshore waters off the Atlantic coast (Schwartz, Heimiller, Haymes, & Musial, 2010).

We focus on optimizing the siting of wind farms since, once installed, the location of a wind farm cannot be adjusted, only its operation (Singh, Baker, & Lackner, 2015). A large portion of the costs related to offshore wind energy occurs during installation, which means that operators want to maximize operating time over the life of the facility and avoid unanticipated curtailment or reduction in efficiency.

As offshore wind farm development grows, so does the potential for interactions between individual wind farms, as well as for cumulative environmental impacts to the surrounding ecosystems. While individual wind farms generally have negligible population level impacts to the surrounding ecosystems, hundreds of wind farms could result in an accumulation of impacts larger than the sum of the individual impacts (Berkenhagen et al., 2010). Large scale wind farm development could lead to tipping points such as cumulative collision mortality rates which reduce a species' long run population or habitat fragmentation caused by wind farms acting as a barrier to movement between essential habitats (Drewitt & Langston, 2006; Hüppop, Dierschke, Exo, Fredrich, & Hill, 2006). Due to the non-linear interactions among wind farm sites in power generation and cumulative environmental impacts, examination of facility siting policies on a larger scale can illuminate improved pathways for large-scale wind farm development. The alternative – considering wind farm siting as a series of independent decisions – cannot properly address the long-term, interdependent nature of these decisions and could result in suboptimal wind farm development with regard to one or more of the objectives. Developing a

* Corresponding author. Present address: Natural and Applied Sciences, Bentley University, 225 Jennison, 175 Forest Street, Waltham, MA 02452, United States.
E-mail addresses: acranmer@bentley.edu (A. Cranmer), edbaker@ecs.umass.edu (E. Baker), juuso.liesio@aalto.fi (J. Liesiö), ahti.salo@aalto.fi (A. Salo).

https://doi.org/10.1016/j.ejor.2017.11.026
0377-2217/

quantitative understanding of how these interactions develop can aid stakeholders in planning for long term renewable energy targets and environmental conservation goals. Thus, we argue that the problem of wind farm siting should be framed as a portfolio problem, evaluating multiple sites simultaneously.

In this context, we address this problem by developing a top-down optimization model that maximizes the economic value of a portfolio of offshore wind farms while respecting environmental constraints. We use a portfolio approach to examine a set of potential offshore wind farm locations collectively instead of individually, and use this model to examine the tradeoffs between economic and environmental outcomes in this spatial multi-criteria problem.

This research differs in two key ways from previous research. First, we focus on siting multi-turbine wind farms, rather than the layout of individual turbines within farms. The wind farm unit is the appropriate unit for a social planner to consider. Existing models of turbine layout are far too computationally complex to be tractable on the order we are considering if each turbine is modeled individually. On the other hand, wind farms cannot be correctly modeled as single large turbines of equivalent capacity, since the wake resulting from a wind farm is larger and more spread out. Therefore, existing turbine layout models cannot be easily adapted to site wind farms.

Second, we develop a novel modeling approach for capturing the spatial interactions of the offshore wind resource. This approach is based on using linear network models to track how the location-specific wind speeds develop as the wind travels through a combination (i.e. a portfolio) of wind farms. By using these networks for all wind scenarios (i.e., free wind speed and direction), we obtain a linear programming formulation for the power generated by an arbitrary portfolio of farms. Moreover, the linearity of the model is preserved when the wind farms to be developed are treated as decision variables. Thus efficient mixed-integer linear programming (MILP) algorithms can be used to identify a portfolio of wind farms that maximizes economic value while satisfying relevant environmental constraints.

The vast majority of the literature focuses on project developers and prescribes the precise location and arrangement of individual wind turbines within farms, what is called micro-siting. This work typically focuses on maximizing power output for a fixed number of turbines. Due to the complexities of fluid flow within a wind farm, virtually all micro-siting models use heuristic approaches to optimize turbine placement (Elkinton, Manwell, & McGowan, 2008; Lackner & Elkinton, 2007; Veeramachaneni, Wagner, O'Reilly, & Neumann, 2012; see González, Payán, Santos, & González-Longatt, 2014 for a review). Recent work using swarm optimization and genetic algorithms provides additional value in micro-siting problems by removing the requirement to site turbines on a grid (Wan, Wang, Yang, Gu, & Zhang, 2012).

Our work, in contrast, is aimed at regulators and policy-makers, and is intended to inform strategic policy and regulatory decisions related to defining wind energy areas and permitting individual wind farms. This aim has important implications for the modeling choices made in this paper. First, the spatial units of analysis used by the U.S. Federal regulatory agencies are gridded points known as blocks or aliquots (we call them sites). Hence, for each of these sites we consider the binary decision of whether or not a wind farm should be developed, rather than treating the coordinates of each wind farm as continuous decision variables. Second, making informed policy decisions requires an equitable treatment of all available decision alternatives. Indeed, our model can be solved with exact MILP algorithms to identify the true global optimal solution among all feasible ones. Heuristics, in turn, would offer no guarantees that the produced solution is the true optimum. In principle, existing simulation models could be used to evaluate the economic values of each possible site combination. However, as the number of combinations increases exponentially in the number of sites, this approach quickly becomes infeasible: For instance, with a relatively modest grid consisting of 10×10 sites, the number of combinations to simulate would be in the magnitude of $2^{100} \approx 10^{30}$.

A few papers have developed mixed-integer linear programs (MILPs) maximizing power in packing-type problems (Archer, Nates, Donovan, & Waterer, 2011; Fischetti & Monaci, 2016; Turner, Romero, Zhang, Amon, & Chan, 2014; Zhang, Romero, Beck, & Amon, 2014). Fischetti and Monaci (2016) consider the context of a large offshore wind farm and combine heuristics with a MILP formulation. Our approach diverges from this previous optimization work as well as from that of Volker, Hahmann, Badger, and Jorgensen (2017) by focusing not on maximizing power output, but on maximizing the profitability of the wind farms. An increase in power output must be evaluated against the additional capital investment required.

Others have taken a portfolio approach to planning wind farms with agents responding to a market for electricity (Le Cadre, Papavasiliou, & Smeers, 2015). Our approach differs in informing the extensive permitting process that is typical for offshore wind farms, and focuses on ex-ante spatial concerns rather than ex-post market concerns. We take the perspective of the social planner, rather than the agents producing and selling energy, since planners and regulators identify development areas for offshore wind projects in the U.S. Our paper can be seen as a complement to this paper.

We take a novel approach to modeling the spatial interactions between discrete wind farm sites in a portfolio decision framework. The sites are discrete by the nature of the policy. For example, each wind energy area (WEA) in the U.S. is composed of Federal lease blocks, which discretize the offshore space designated for leasing. We develop a network model within the optimization to track how siting decisions impact power generation at downwind farms. This allows us to linearize nonlinear relationships for a discretized space and solve large problems quickly. It incorporates the variability in wind by modeling the frequency over a set of wind scenarios with different wind speeds and wind directions (Baker & Solak, 2011; Liesio & Salo, 2012; Liesio, Mild, & Salo, 2008). The model is computationally attractive because it is a MILP model which can be readily solved for problem sizes relevant to practical problems.

This paper also contributes to the Portfolio Decision Analysis (PDA) literature. Specifically, PDA refers to the theory, methods and practices which seek to help decision makers make informed *multiple* selections from a discrete set of alternatives (for an overview see, e.g., Salo, Keisler, & Morton, 2011). Indeed, the approach developed here demonstrates how complex spatial interactions and uncertainties can be efficiently captured in a portfolio model of practical relevance. In line with PDA literature, we use the term 'portfolio' to refer to a combination of decisions on whether or not a wind farm is developed on each site. It is worth highlighting that financial portfolio models (e.g., Markowitz, 1952) which seek to balance return and risks through diversification have a different purpose: In these models, portfolio refers to the allocation among different (market traded) financial assets.

The remainder of this paper is organized as follows. Section 2 develops the model for optimizing the arrangement of wind farms. Section 3 presents an application using wind data from the Gulf of Maine and explores the effect of restricting environmental corridors from wind farm development. Section 4 shows how the model can be extended to capture wind dynamics through a more precise model. Section 5 discusses the insights that the model can provide for public officials responsible for reviewing offshore wind farm permit applications

as well as for energy companies that plan and develop wind farms.

2. Model for optimizing the portfolio of wind farms

We start by establishing the notation and defining the objective function in Section 2.1. Section 2.2 describes the network for modeling the power generation and the profits of the wind farms. The environmental objective and constraints are described in Section 2.3. Finally, the full model is presented in Section 2.4.

2.1. Notation

The model is designed to select optimal locations for wind farms within a region. The possible locations for building wind farms are identified by grid points $(x, y) \in G = \{1, 2, \ldots, \bar{x}\} \times \{1, 2, \ldots, \bar{y}\}$ where (1,1) is the lower left corner of the grid and parameters $\bar{x}$ and $\bar{y}$ define the size of the grid. The wind farm portfolio is represented by Z, an $\bar{x}$ by $\bar{y}$ matrix with binary elements: $z_{x,y} = 1$ if a wind farm is built at coordinates (x, y) and 0 otherwise.

The model includes a set of eight network models designed to capture wind directions over bins of 45° angles each, centered around the direction $a \in A$. Each network aggregates the behavior of nine 5° wind direction bins (Appendix A). For each direction $a \in A$, there is a set of scenarios $\omega \in \Omega^a$ defined by $u_0(\omega)$, the free stream wind speed from the direction in scenario ω, and the corresponding frequency of a particular wind scenario, denoted by $f(\omega) \in [0, 1]$. These frequencies sum to one: $\sum_{\omega \in \Omega} f(\omega) = 1$ where $\Omega = \cup_{a \in A} \Omega^a$ denotes the set of all wind scenarios across all directions. For instance, $\omega \in \Omega^{left}$ such that $u_0(\omega) = 8$ and $f(\omega) = 0.2$ would correspond to a wind scenario with eight meters per second wind coming from the left side of an area, which occurs 20% of the time.

Let $P(\omega, Z)$ capture the power output generated by wind farms under wind scenario $\omega \in \Omega^a$. The total *expected* power output over all wind scenarios (i.e. speeds and directions) is then

$$\bar{P}(Z) = \sum_{a \in A} \sum_{\omega \in \Omega^a} f(\omega) P(\omega, Z) \tag{1}$$

Assuming that the power function P is known, the economically optimal wind farm portfolio can be identified by solving the mixed integer programming problem

$$\max_{Z} \left(Rh\upsilon \bar{P}(Z) - \sum_{(x,y) \in G} C_{x,y} z_{x,y} \right), \tag{2}$$

which maximizes the total profits from the portfolio of wind farms. Specifically, in Problem (2) the parameter R is the revenue rate for energy in dollars per kilowatthour and h is the operating hours per year. Power $\bar{P}$ multiplied by hours h gives the average annual energy produced by the wind farm, which is measured in kilowatthours. This is then multiplied by a present value factor, υ, defined as $\upsilon = ((1+r)^m - 1)/(r(1+r)^m)$ where r is the discount rate, and m is the lifetime of the wind farm in years. The overnight capital cost[1] for a wind farm at coordinates (x, y) in U.S. dollars is represented by $C_{x,y}$.

2.2. Capturing wake effects with a network-flow model

Developing a wind farm at a particular site reduces the wind speed and available power at the next downwind site, while an undeveloped site allows for the wind to rebound (but never above the initial free stream value). A network-flow model captures the nonlinear interdependency between power output, wind speed, and the location of wind farms. Section 2.2.1 briefly describes the wake decay functions used to establish the power output levels in the network model. Section 2.2.2 develops the model for the power output $P(\omega, Z)$ in a scenario with wind from the left side of the area, i.e. $\omega \in \Omega^{left}$, where left could represent west or another direction depending on how the area of interest is oriented relative to the directions. The same model can apply to the other wind directions with only minor modifications as discussed in Section 2.2.3. Section 2.2.4 discusses extensions to account for wind along the diagonal directions.

2.2.1. Wake decay functions

To parameterize the model, we need to establish power output levels in the model. We consider two different wind speed decay functions which represent different meteorological conditions that result in greater or lesser interactions between wind farms through wake effects. Let d represent the size of the windfarm, specifically in terms of the distance between the first and last row of turbines. Then, the wind speed exiting a farm of size d is given by $u(d) = u_0 \beta(d)$, where the decay factor $\beta(d)$ takes one of the two functional forms

$$\beta(d) = d^{-\gamma}, \tag{3}$$

$$\beta(d) = e^{-\alpha d}. \tag{4}$$

Parameters γ and α correspond to the function for wind speed through the wind farms with low (high) decay (see Appendix A for more detail). These functions fit published wake data for a large offshore wind farm (Barthelmie et al., 2009), but have different implications for larger areas. The goal of these functions is to simply and appropriately model the interactions between wind farms in terms of power output. They are in line with the results of Volker et al. (2017), which were derived using more complicated wind flow simulations. The form of the wake model has no impact on the structure of our model. It is only used to assign wind resource values to the levels in the network model (Fig. 1).

2.2.2. The power output function for one wind scenario

Let $\omega \in \Omega^{left}$ be a wind scenario with free stream wind speed $u_0(\omega)$ and $y \in \{1, \ldots, \bar{y}\}$ be a row coordinate. Furthermore, assume that a wind farm reduces the wind speed by a factor of $\beta(d)$. Then the wind speed at any of the coordinate points $(1, y), \ldots, (\bar{x}, y)$ is an element of the vector $(u_1(\omega), \ldots, u_{\bar{x}}(\omega)) = u_0(\omega) * (1, \beta(d), \beta(2d), \ldots, \beta((\bar{x}-1)d))$. Note that we use $i = 1, \ldots, \bar{x}$ as indices for the wind speed vectors $u_i(\omega)$, since there are exactly $\bar{x}$ possible wind speeds in the row of sites. An undeveloped site allows the wind speed to rebound from $u_i(\omega)$ to $u_{i-1}(\omega)$ at the next site. Let $\rho_i(\omega)$ represent the power generated by an individual wind farm given wind speed $u_i(\omega)$; and then any site developed in coordinate points $(1, y), \ldots (\bar{x}, y)$ generates power equal to an element of the vector $(\rho_1(\omega), \ldots, \rho_{\bar{x}}(\omega))$.

To determine which of these elements corresponds to the actual power output at a specific site requires knowledge of (i) the incoming wind speed distribution and (ii) whether or not a wind farm is built. For this purpose, define binary variables $\theta^+_{ji}(\omega, y)$ and $\theta^-_{ji}(\omega, y)$ where $j = \{1, \ldots, \bar{x}\}$ represents sites (within row y) and $i \in \{1, \ldots, j\}$ represents the element of the wind speed vector:

- $\theta^+_{ji}(\omega, y) = 1$ if the wind speed is $u_i(\omega)$ *and* site j is undeveloped; and 0 otherwise;
- $\theta^-_{ji}(\omega, y) = 1$ if the wind speed is $u_i(\omega)$ *and* site j is developed; and 0 otherwise.

[1] Overnight capital cost refers to the sum of project construction costs without interest, i.e. if it were possible to build it "overnight" (U.S. Energy Information Administration, 2013).

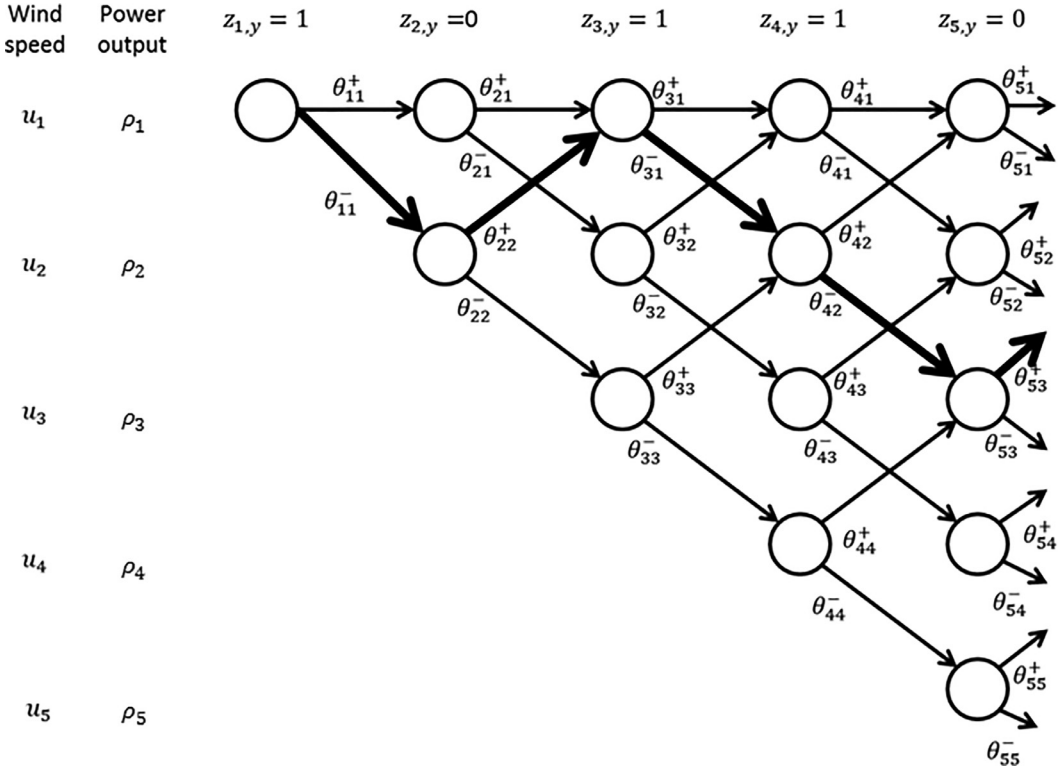

Fig. 1. Network flow model for the wind. Bolded arrows indicate variables such that $\theta_{ji}(\omega, y) = 1$ given decision variable values $z_{:,y} = (1, 0, 1, 1, 0)$. The wind speed distributions at the five sites are u_1, u_2, u_1, u_2, u_3 and hence the total power output (1) is equal to $\rho_1 + 0 + \rho_1 + \rho_2 + 0$.

These variables can be interpreted as network flow variables of the binomial lattice illustrated in Fig. 1. When $\theta^+_{ji} = 1$ this implies that the wind speed in site $j+1$, is increased or stays unabated; when $\theta^-_{ji} = 1$ this implies that the wind speed in site $j+1$ is decreased. When they are both zero, this implies that the wind speed entering site j is not equal to $u_i(\omega)$.

The sum of the initial binary variables must be one: that is, the wind leaving the first site must be either equal to the free stream wind or equal to $u_2(\omega)$, i.e.

$$\theta^+_{11}(\omega, y) + \theta^-_{11}(\omega, y) = 1. \tag{5}$$

Furthermore, we need to ensure that the flow into each node equals the flow out of the node, implemented by the following constraints

$$\theta^+_{11}(\omega, y) = \theta^+_{21}(\omega, y) + \theta^-_{21}(\omega, y) \tag{6}$$

$$\theta^+_{j-1,1}(\omega, y) + \theta^+_{j-1,2}(\omega, y) = \theta^+_{j,1}(\omega, y) + \theta^-_{j,1}(\omega, y) \ \forall j = 3, \ldots, \bar{x} \tag{7}$$

$$\theta^+_{j-1,i+1}(\omega, y) + \theta^-_{j-1,i-1}(\omega, y) = \theta^+_{j,i}(\omega, y) + \theta^-_{j,i}(\omega, y) \quad \forall j = 4, \ldots, \bar{x}, \ i = 2, \ldots, j-2 \tag{8}$$

$$\theta^-_{j-1,j-1}(\omega, y) = \theta^+_{j,j}(\omega, y) + \theta^-_{j,j}(\omega, y) \ \forall j = 2, \ldots, \bar{x} \tag{9}$$

$$\theta^-_{j-1,j-2}(\omega, y) = \theta^+_{j,j-1}(\omega, y) + \theta^-_{j,j-1}(\omega, y) \ \forall j = 3, \ldots, \bar{x}. \tag{10}$$

Constraints (6) and (7) ensure a network structure that does not permit the wind speed to rebound above the original free stream value. Finally, we link the route through the network to the decision of whether or not a site will contain a wind farm via the $\theta^-_{ji}(\omega, y)$ variables:

$$z_{j,y} = \sum_{i=1}^{j} \theta^-_{ji}(\omega, y) \ \forall j = 1, \ldots, \bar{x}. \tag{11}$$

If any one of these $\theta^-_{ji}(\omega, y)$ variables equals one, then site j has a wind farm and we can generate power from grid point (j, y). When $z_{j,y} = 1$, site (j, y) can produce $\rho_i(\omega)$, the power associated with the i value of the variable $\theta^-_{ji}(\omega, y)$ which equals one. Otherwise, $z_{j,y} = 0$ and the site cannot produce power. Hence, total power from the row of sites $z_{1,y}, \ldots, z_{\bar{x},y}$ can be obtained as the sum

$$\sum_{j=1}^{\bar{x}} \sum_{i=1}^{j} \theta^-_{ji}(\omega, y)\rho_i(\omega).$$

Fig. 1 shows an example of how the Z and P variables are linked to the flow variables $\theta_{ji}(\omega, y)$ when wind farms are built on the first, third and fourth sites a specific row. The same model can be repeated for each row, y, with each parallel set of sites having a distinct set of variables $\theta^+_{ji}(\omega, y)$ and $\theta^-_{ji}(\omega, y)$. The total power under wind scenario $\omega \in \Omega^{left}$ is then obtained from

$$P(\omega, Z) = \sum_{y=1}^{\bar{y}} \sum_{j=1}^{\bar{x}} \sum_{i=1}^{j} \theta^-_{ji}(\omega, y)\rho_i(\omega). \tag{12}$$

2.2.3. The power output functions for other wind scenarios

For a wind scenario $\omega \in \Omega^{top}$, the power produced by a column of sites in grid points $(x, \bar{y}), \ldots, (x, 1)$ the model for power output is almost identical to (12). The only difference is that since the binary variables $\theta^+_{ji}(\omega, x)$ and $\theta^-_{ji}(\omega, x)$, $i \in \{1, \ldots, j\}$ capture the wind speed changes to the j:th site *downwind*, they must be linked to the decision variables indicating whether or not to develop the site at grid point $(x, \bar{y} + 1 - j)$. Hence

$$z_{x,\bar{y}+1-j} = \sum_{i=1}^{j} \theta^-_{ji}(\omega, x), \ \forall j = 1, \ldots, \bar{y} \tag{13}$$

replaces constraint (11). These are identical except that y in (11) is replaced with x in (13) and the indices i and j index rows rather

than columns. The power output becomes

$$P(\omega, Z) = \sum_{x=1}^{\bar{x}} \sum_{j=1}^{\bar{y}} \sum_{i=1}^{j} \theta_{ji}^{-}(\omega, x)\rho_i(\omega) \tag{14}$$

For a wind scenario $\omega \in \Omega^{right}$ or $\omega \in \Omega^{bottom}$, the corresponding equations for the decision variables are, respectively,

$$z_{\bar{x}+1-j,y} = \sum_{i=1}^{j} \theta_{ji}^{-}(\omega, y), \ \ \forall j = 1, \ldots, \bar{x}$$

$$z_{x,j} = \sum_{i=1}^{j} \theta_{ji}^{-}(\omega, x), \ \ \forall j = 1, \ldots, \bar{y}$$

The power output functions for the scenarios are the same as (12) and (14), respectively.

2.2.4. Modeling diagonal wind directions

We model the diagonal wind directions similar to the wind directions above except that there are three upwind farms which can impact a downwind farm. Each upwind neighbor can contribute one third of a level of decay to their diagonal downwind neighbor. As above, each site is represented with a set of nodes and each node has only two arcs extending from it, indicating the decision to build or not to build a wind farm. Unlike the networks for the non-diagonal wind directions, rebound can occur only through the primary diagonal sites (defined in Appendix B) and not through the secondary diagonal sites which can contribute to the decay. If a primary diagonal site is left open, a full level of rebound occurs. Furthermore, only the arcs associated with building wind farms in the primary diagonal sites have nonzero profit values. The modifications to describe power output along the diagonals is described in Appendix B.

2.3. Including environmental objectives

The environmental objectives for siting wind farms can include maximizing the distance of the facilities from sensitive habitats, such as nesting and breeding sites, and maximizing the continuous area of open space around the wind farms, i.e. minimizing the fragmentation of sensitive habitat areas. In this paper we take a simple approach to this objective by restricting certain sets of sites from wind farm development. Restricting the columns of sites with indices in the set $m_x = ((x, 1), \ldots, (x, \bar{y})), \ \ x \in \{1, \ldots, \bar{x}\}$ requires introducing the additional constraints

$$z_{x,y} = 0, \ \ \forall x \in m_x. \tag{15}$$

We use a similar constraint if we want to restrict rows of sites.

These constraints can represent important ecological corridors, for example the shortest paths between nesting and feeding areas. We use these constraints to investigate the tradeoffs between value for energy production and different strategies for ecologically sensitive wind farm development.

Another approach to limiting environmental impacts in areas of highly sensitive ecological activity, is to limit the total number of projects in a sensitive area. This can be implemented by introducing the constraint

$$\sum_{x=1}^{\bar{x}} \sum_{y=1}^{\bar{y}} z_{x,y} \leq \bar{N} \tag{16}$$

where $\bar{N}$ denotes the maximum number of wind farms. As the permitted density of wind farms decreases, the need for quantitative modeling decreases because the available wind farm sites become few and their interactions much less significant.

2.4. The complete model

Substituting the power output functions $P(\omega, Z)$ developed above in Eqs. (12) and (14) into the original model for profit maximization, results in the following mixed integer programming model

$$\max_{Z \in \{0,1\}^{\bar{x} \times \bar{y}}} \left(Rh\upsilon \bar{P}(Z) - \sum_{(x,y) \in G} C_{x,y} z_{x,y} \right)$$

$$\bar{P}(Z) = \sum_{a \in A} \sum_{\omega \in \Omega^a} f(\omega) P(\omega, Z), \ \ where$$

$$z_{x,y} = 0, \ \ x \in m_x$$

$$z_{x,y} = 0, \ \ y \in m_y$$

$$\sum_{x=1}^{\bar{x}} \sum_{y=1}^{\bar{y}} z_{x,y} \leq \bar{N} \tag{17}$$

3. Application to Gulf of Maine

In this section, the model developed in Section 2 is applied to examine the optimal siting of wind farms in a 10 × 10 grid of possible sites in the Gulf of Maine. Located off the North Atlantic coast of the United States, the Gulf of Maine has been considered by developers for installing offshore wind farms.

3.1. Data for portfolio model

3.1.1. Wind data

The Gulf of Maine has a nearby data buoy maintained by the National Oceanic and Atmospheric Administration (NOAA) with many years of wind data available, of which we use 1994 through 2014 data (National Data Buoy Center, 2015). We use the power law to extrapolate the hub height wind speeds from the buoy data (Manwell, McGowan, & Rogers, 2009; Schwartz et al., 2010). Fig. 2 shows the distribution of wind speeds for each direction at a hub height of 90 meters. The length of the cone in each direction indicates the frequency of each direction, for example, there's an almost 18% chance of wind from the SW. Within each direction, the coloring indicates the cumulative frequency of wind speeds, for example, there's a 9% chance that wind will come from the NE at less than 20 meters per second.

A power curve defines the relationship between wind speed and power output for a particular type of wind turbine, as shown in Fig. 3. The turbine operates at wind speeds above the cut-in speed and below the cut-out speed. Power out increases cubically with the wind speed until the rated wind speed and power are reached. Above the rated wind speed, power output remains constant. We take the distributions from Fig. 2 and convert the wind speeds into power outputs via the power curve.

At low wind speeds, the revenue generated cannot compensate for the capital costs of development. In these cases, the best choice is not to develop any wind farms. At medium wind speeds, enough revenue is generated to recoup the capital costs; however, when wind speeds are in the cubic section of the power curve, the wind farms are very susceptible to the impacts of wake effects from any neighboring farms. At high wind speeds, above the rated wind speed, the power output is constant, so in these cases the wind farms are less impacted by wake effects from any neighbors.

Most areas have a prevailing wind direction, which in the Gulf of Maine is the southwest, so we orient the grid of sites so that one edge faces the southwest direction. The prevailing wind direction is consistent across the U.S. Atlantic coast and the wind speed profile changes very slowly, so we can take this wind speed profile for a large area such as that considered in this paper with minimal error. If the area considered were larger than the coastal area

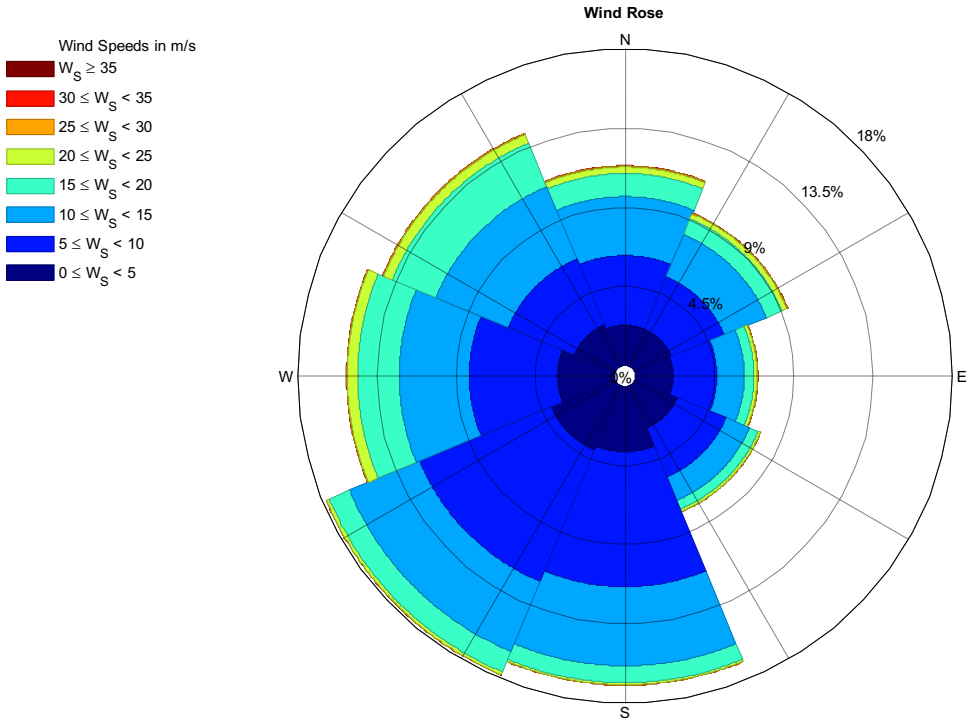

Fig. 2. Wind speed distribution for eight wind directions. There is an almost 18% chance that wind will come from the SW and about half of that time it will be between 5 and 10 meters per second. (For interpretation of the references to color in this figure, the reader is referred to the web version of this article).

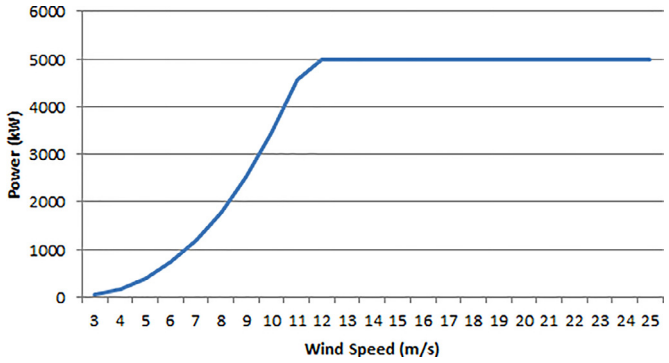

Fig. 3. Power curve for 5 megawatt reference turbine (Jonkman et al., 2009). https://wind.nrel.gov/forum/wind/viewtopic.php?t=363.

of the state of Maine, some corrections for changes in the wind speed profile may become necessary.

3.1.2. Wind farm characteristics

In this application, we use wind farm units of nine 5 megawatt NREL reference turbines (Jonkman, Butterfield, Musial, & Scott, 2009) with a ten rotor diameter spacing, for a capacity of 45 megawatts in an area of ≈14.3 square kilometers. To use the MILP model in (17), we define the power outputs $\rho_1, \ldots, \rho_n$ for the possible wind speed distributions $u_1, \ldots, u_n$ as described in Eq. (3) in the previous section. From the literature discussed in Appendix A, we estimate $\gamma \approx 0.063$, which results in an 18% reduction after the first farm for winds approaching perpendicular to the edge of a wind farm. Using this, we calculate different wind speed levels based on the free stream wind speed and use the power curve, shown in Fig. 3, to obtain power output levels.

We estimate the power produced in 5° direction bins and aggregate them into expected power for the eight directions included in the model. The expected power of each wind speed distribution, u_1, is then used as the freestream expected power output, ρ_1, for the associated wind direction. Based on data available in the literature, we estimate a decay function for the wind speed as it passes through a series of wind farms (Barthelmie et al., 2009; Gaumond et al., 2014; Jimeńez, Navarro, Palomares, & Dudhia, 2015; Peña, Réthoré, & Rathmann, 2014; Walker et al., 2016). More details are provided in Appendix A. In order to find the ρ_2 values for each direction, each wind speed data point is subjected to the decay function (3) and a new wind speed distribution is found for a downwind farm, u_2. Again, the expected power, ρ_2, is found for each direction. This procedure is repeated until ρ_n is reached, where $n = \max\{\bar{x}, \bar{y}\}$.

Power output is converted to a profit value by calculating the net present value over twenty years of operation with a social discount rate of 3%. The revenue calculation assumes a power purchase agreement for 0.20 dollars per kilowatthour and overnight capital costs of 6230 dollars per kilowatt (U.S. Energy Information Administration, 2013). For simplicity, we assume uniform capital costs across all sites; however, in reality the capital costs of sites will likely differ though these relationships remain unclear as technology evolves, and companies and regulatory agencies learn from earlier U.S. projects. It is straightforward to modify the model presented here to give each site a different capital cost or to allow neighboring sites to share cable infrastructure through the network structure.

3.2. Computation

For the wind directions perpendicular to an edge of the area, each row or column of sites has 110 network (θ) variables from Eqs. (5)–(10) and 55 constraints. For the wind directions along the diagonals of the area, a series of different size networks totals 20,672 network variables and 11,632 constraints. The model also includes 100 z-variables, one for each site in the area and each scenario includes 200 consistency constraints which require the model to choose the same sites in each scenario. Thus the model

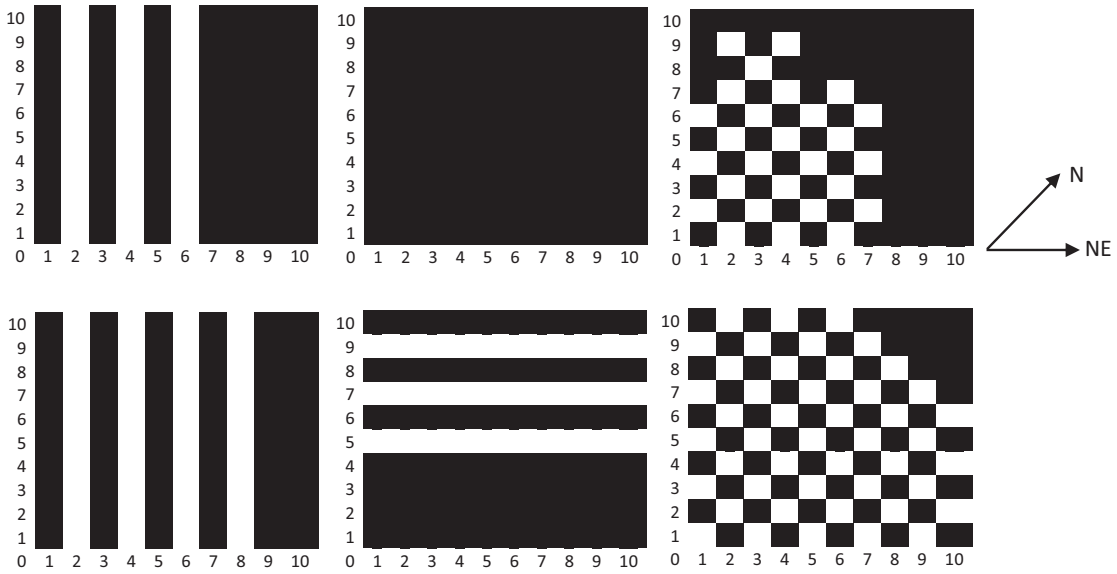

Fig. 4. Optimal layout for winds from the southwest direction only (left panels); northwest only (middle panels); and equally distributed from the southwest and southeast winds (right panels). The top row assumes low decay (3); the bottom row assumes high decay (4).

for a 10 × 10 grid has a total of $4400 + 20{,}672 + 100 = 25{,}172$ variables (θ's and z's) and a total of $2200 + 11{,}632 + 1400 = 15{,}232$ constraints.

The model was implemented in Matlab and used Gurobi to solve the MILP problem. The eight wind direction scenario problem described above takes from seconds to a few days, depending on the decay function and the constraints placed on the problem. We consider this quick relative to the planning horizon and lifetime of an offshore wind project, which takes years to plan and has a lifetime of 20–30 years. The low decay cases solved more quickly than the high decay cases. Each reference case (Fig. 5) took 1.5 seconds and 37 hours, respectively, on a computer with a quad core 3.40 gigahertz processor with 8 gigabytes of RAM. In both cases, the maximum run time occurred while solving with a site budget constraint, almost 4 days for the low decay case and 8 days for the high decay case.

3.3. Results

In this section, we describe the results and present optimal wind farm layouts under different wind conditions, showing wind farms as black squares and open space as white squares. The results show how the different wind speeds and wind directions influence the placement of wind farms and give a sense of the underlying mechanics of the model and development of the optimal solution. Subsequent sections discuss results with siting restrictions (3.4) and the value of this portfolio approach to siting offshore wind farms (3.5).

When the wind speeds are mostly between the cut-in and rated wind speeds, as in the case of winds from the southwest, the top left of Fig. 4 shows the results. This panel shows the optimal arrangement of wind farms if wind only came from the southwest at the distribution observed for that direction in the data. The wind farms are arranged such that the wind speeds can rebound between columns of wind farms, allowing the wind farms to produce their maximum power all the time. The only exception is the eighth and tenth columns, which are part of an edge effect that occurs because there are no sites to consider beyond the tenth column of sites. The panel below (bottom left) shows the optimal arrangement assuming the higher decay function, holding everything else constant. The difference between the two shows how the increase in interactions affects the optimal solution – more sites are left open (column 8) and the downwind edge effect is smaller. If the area under consideration were larger, the alternating columns pattern would continue up to the last two columns, which would exhibit the edge effect.

In a case where the frequency of wind speeds above the rated speed is high, such as in the case of winds from the northwest, we see a higher density of wind farms. The middle panels show the optimal layout if wind only came from the northwest with the wind speed distribution observed for the direction given low interactions (top) or high interactions (bottom). In these cases, the higher wind speeds reduce the interactions between sites in terms of power and profit, countering the benefits of foregoing wind farms so more sites are chosen for wind development. At high wind speeds, the power output of the turbine does not decline with the wind speed, so the wakes have less impact on the profitability of the wind farms.

In the case of wind from the south only (not shown in the figure), the diagonal direction means a larger spacing between the turbines, and the decay is correspondingly reduced and again all wind farm sites are chosen.

In the case of two wind directions with high frequencies of medium wind speeds, such as in the case of winds from the southwest and southeast with equal probabilities, we see how the alternating rows and columns of wind farms are combined to form a checkerboard pattern from the most upwind corner of the area through the center of the area (right side panels of Fig. 4). The most downwind corner shows an edge effect as the number of downwind sites becomes very small. Both the southwest and southeast wind directions have low frequencies of high wind speeds, making the overall density of wind farms relatively low. In cases with higher frequencies of high wind speeds, the density of wind farms will be higher, the checkerboard patterned area will be smaller and the downwind edge effect will be larger.

In some cases, the symmetry of the wind conditions and the results indicate multiple optimal solutions; however, this seems confined to certain cases with high levels of symmetry in wind direction, wind speed, and probabilities of each.

Ignoring electrical grid connections and environmental considerations, the optimal wind farm layout for all eight wind directions using the Gulf of Maine data results in most or all sites de-

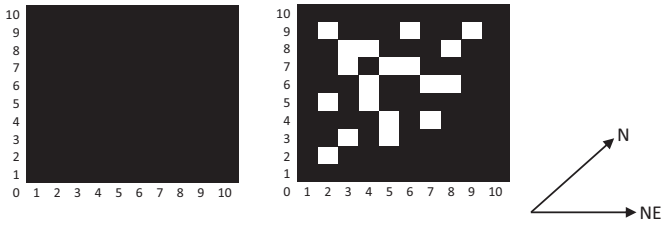

Fig. 5. Wind farm layout results based on eight wind directions with low decay (left) and high decay (right) functions.

veloped, depending on the assumptions about the decay function (Fig. 5). Given the high wind speeds seen in the Gulf of Maine, the losses between sites are insufficient to warrant foregoing any development if the interactions between the sites are low, so all sites are chosen for wind farms (left panel). Assuming higher interactions it is worth foregoing almost one fifth of sites to maximize the profitability of all sites collectively. In general, an area with a lower frequency of high wind speeds would have an optimal layout with a lower density of wind farms. Furthermore, given the existing uses of the offshore space, not all sites can be developed. Consequently, it is important to consider the portfolio of offshore wind farms with a constraint on the location or number of permitted sites, which we turn to in the next section.

3.4. Ecological restrictions

If regulators want to restrict certain sets of sites from wind farm development because, for instance, they are defined as ecological corridors, our model can assess the impacts of these restrictions on the economic value of the sites for offshore wind energy. As restricted corridors increase or become wider, as shown in Fig. 6, the optimal profit value decreases as shown in Fig. 7. The losses increase as the number of sites restricted from wind farm development increases and the losses are slightly higher when the restricted areas are all adjacent to each other. The losses are higher for corridors aligned with the prevailing wind direction as opposed to those perpendicular to the prevailing wind. Aligning corridors perpendicular to the prevailing wind direction more closely resembles the optimal solution in the left most panels of Fig. 4.

Restricting sites from wind farm development has a nonproportional impact on the total value of the sites: making half of the sites unavailable for wind farm development results in total value losses of less than half because the open area leaves wind resources available to the other sites which are still available for wind farm development.

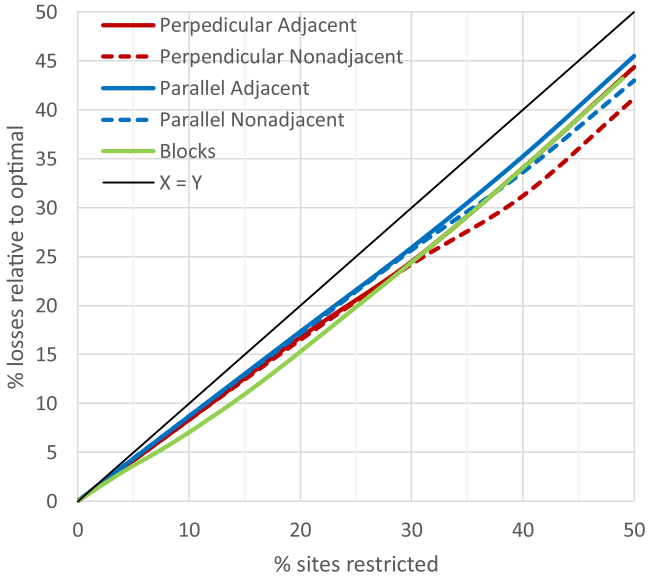

Fig. 7. Impacts of environmental restrictions on total profit values.

3.5. Value of the portfolio approach

To demonstrate the value of the portfolio approach, we compare the results of our model with those from two heuristics: a no planning model and a myopic planning model. The no planning model implies that there is no social planner; developers choose each project only to maximize their own profits. The myopic planning model selects the next site based on its own economic value *and* its impact on existing wind farms; this represents a planner who only reacts to each new wind farm, rather than planning ahead. All three models are solved for a range of values for the number of permitted sites.

Both models begin by assessing the economic value of the available sites. In the case of the myopic planning model, an additional step calculates the total value of all existing sites with each of the candidate sites. In many cases, both models find multiple maximizing choices; in these cases, the models choose at random and we run each model 50 times. The no planning model will continue to add wind farms until there are no more positive valued farms. The myopic planning model adds new wind farms until an additional wind farm has a net negative economic effect on the portfolio of wind farms.

With no external constraint on the percent of permitted sites, both the no planning and myopic planning models develop all

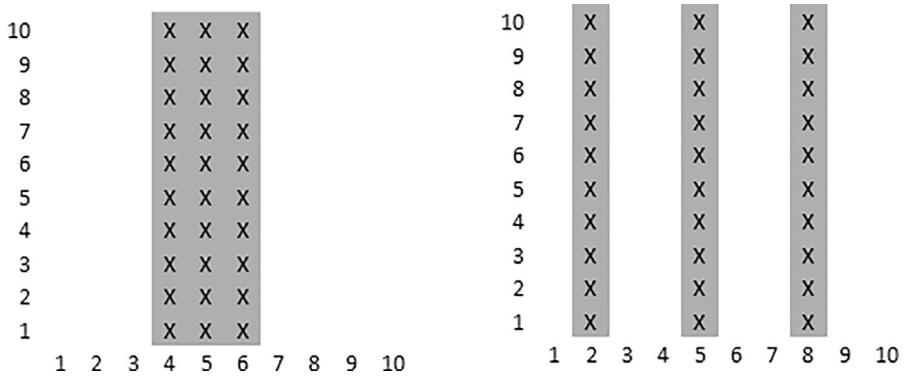

Fig. 6. Examples of site restrictions (areas marked with X) for environmental corridors, a corridor with width of three adjacent columns (left) and three nonadjacent restricted columns (right).

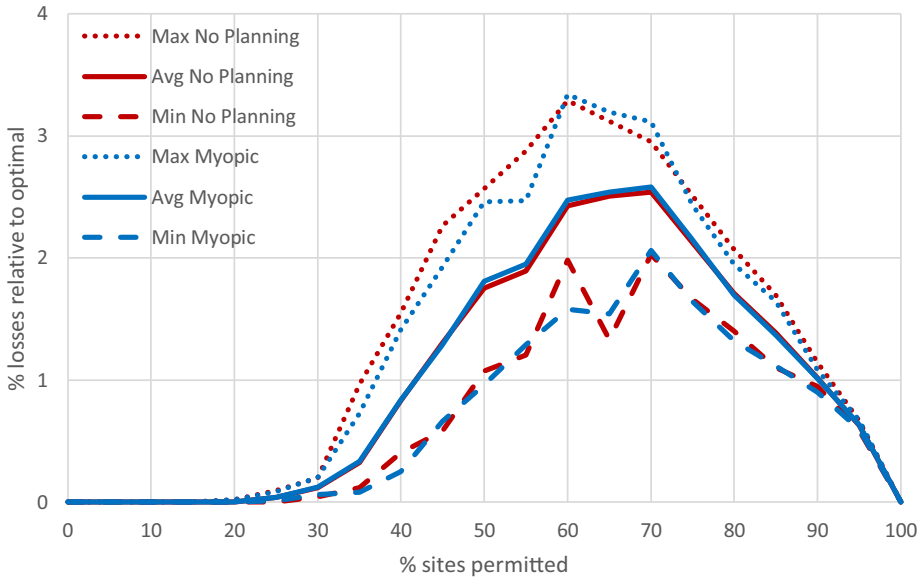

Fig. 8. Loss relative to the optimal for the no planning and myopic solutions, as a function of the percentage of sites restricted. The vertical line indicates where the optimal solution occurs.

sites; however, depending on the percent of permitted sites these heuristics perform as much as 2–3% worse than the portfolio model's optimal solution. In a sensitivity case of greater interactions, described in Appendix A and C, the lost value can be as much as 6%. For billion-dollar offshore wind projects, this would mean hundreds of millions of dollars of lost net present value.

Fig. 8 shows the losses from the best and worst performance over 50 runs of the no planning and myopic models under different constraints on total development. When sites are severely restricted, either heuristic can match the optimal portfolio value by selecting new sites which are not adjacent to existing sites. At the other extreme, if there are no restrictions on sites, then in Gulf of Maine assuming low interactions, all sites are developed so there is no value to the portfolio model.

In between these extremes, however, the portfolio model performs better than the heuristics, by carefully placing wind sites when adjacent sites are needed. In these cases, under the assumption of low interactions shown in Fig. 8, the portfolio model improves on the heuristic solutions by at least 1.5–3%. Under the assumption of high interactions, the improvement can be as much as 6%. For billion-dollar offshore wind projects, this would mean hundreds of millions of dollars of lost net present value. If offshore wind energy is going to contribute to the energy system in a significant way, our model can add value to the long term planning process ensuring that both the developers and electricity consumers get the best possible outcome.

4. Extensions

Here we discuss how assumptions about costs, electrical infrastructure, the wake model, and the shape and size of the wind farms and wind area impact the results of the model.

The model can easily accommodate modifications in the costs of offshore wind farms in terms of distance from shore and electrical cable costs. Here, we have assumed the same capital costs across sites, however, sites which are further from shore or in deeper water may have higher capital costs. The values of $C_{x,y}$ in Eq. (2) can be modified to reflect anticipated capital costs at different locations. We have held these factors constant for simplicity, allowing more straightforward explanations of the results of the model.

Further, the network structure used for the wake effects between wind farms could also be used to model cost synergies between wind farm proximity and electrical infrastructure costs by adding an additional dimension to the values assigned to each level in the network (Fig. 1). Alongside the power output values, ρ_i, we could add the marginal electrical connection cost multiplier, l_i. The vector of multipliers l_i would be very similar to the vector of power: l_i refers to the multiplier when the farm is the ith consecutive farm in a row. The vector of l_i parameters is such that l_1 is equal to 1; with each additional neighboring site, the additional electrical infrastructure costs decrease (i.e. $1 > l_2 > l_3 > \ldots$) because neighboring sites could share some of the equipment and the expenses. Space between wind farms would increase the cost of electrical infrastructure due to the additional cable required and reduced opportunities to share equipment. The first wind farm will pay the full base cost for electrical infrastructure, but a second neighboring farm would have a reduced cost multiplied by l_2. If these two sites were not neighboring, then both would pay the full base costs. A single wind farm near, but not next to, a big cluster of farms could also see reduced costs, but not as much as if it were part of the cluster. The total electrical infrastructure costs $L(Z)$ are obtained in a similar way as the power output values, i.e.,

$$L(Z) = \frac{1}{2}\sum_{x=1}^{\bar{x}}\sum_{j=1}^{\bar{y}} s_{x,j}\sum_{i=1}^{j}\theta_{ji}^{-}\left(\omega^{left}, x\right)l_i + \frac{1}{2}\sum_{y=1}^{\bar{y}}\sum_{j=1}^{\bar{x}} s_{j,y}\sum_{i=1}^{j}\theta_{ji}^{-}\left(\omega^{bottom}, y\right)l_i, \tag{18}$$

where $s_{x,y}$ is the base electrical infrastructure cost for a single wind farm at site (x, y), and $\omega^{left} \in \Omega^{left}$ and $\omega^{bottom} \in \Omega^{bottom}$ are single scenarios with wind coming from the left or the bottom of the area, respectively. Recall that the θ_{ji}^{-} is an indicator of whether a wind farm is installed in site j with power output indexed by i. Existing constraints in the model require consistency of the θ_{ji}^{-} variables across scenarios, so in all the scenarios across a single direction they will be the same across wind scenarios, thus the need for just one scenario from each direction. We sum the electrical costs across all sites and average between the two directions, from the left across rows, and from the bottom across columns. These two directions will give a satisfactory assessment of wind farm proximity.

The objective function is modified to include these additional considerations as follows:

$$\max_{Z\in\{0,1\}^{\bar{x}\times\bar{y}}} \left(Rh\upsilon\bar{P}(Z) - L(Z) - \sum_{(x,y)\in G} C_{x,y}z_{x,y} \right). \tag{19}$$

Thus, the addition of electrical infrastructure costs does not add variables or constraints to the model.

The ratio of the wind speed decay rate to the rebound rate drives the size of the impact radius of a wind farm and the spacing between wind farms in the results. The network model can be adjusted to accommodate different relationships between decay and rebound rates. We assumed a symmetrical, 1:1 relationship between decay and rebound. If this assumption does not hold, the network described in Section 2.2.2 may require additional rows, leading to an increase in the number of variables and constraints for the same size area.

We modeled wind farms of nine turbines arranged in a 3×3 square area, but the structure and underlying dynamics of the model from Section 3.3 would not change for any windfarm layout or size of the model. Rather it is the total number of sites that is important. We modeled an area with 100 possible sites in a 10×10 grid. Adding an additional column or row of sites to the model increases the number of variables in the network (Section 2.2.2) by $\bar{x}$ and adds $2\bar{x}$ constraints.

5. Discussion and conclusions

In this paper, we have formulated a model that represents the complex spatial relationships between decision variables, in this case locations for wind farms, in a tractable way. Our innovation is to represent the impacts of wind farm development on the wind resource as a network flow model. This allows us to solve a complicated spatial planning optimization problem at realistic scales with reasonable computational resources. From this, we can investigate the tradeoffs inherent in siting wind farms as well as the value of planning ahead.

The results of the model can be interpreted in terms of the density of development in different areas, suggesting that planners may want to create offshore zones where higher or lower density wind farm development is permitted. More upwind areas, such as those closer to shore in the case of the U.S. Atlantic coast, would be zoned for lower density development. More downwind areas, further from shore, would be zoned for higher density development.

This model allows planners to consider the costs (in terms of lost profit) of excluding areas from offshore wind energy development. These costs can be compared with the value of the alternate uses such as fishing, shipping, and conservation. In the context of high density, large-scale wind farm development, the potential tradeoffs with ecological conservation depend nonlinearly on the number of sites restricted from potential wind farm development and how those sites are oriented to the prevailing wind direction. The cost increases with the number of sites that are restricted, but this is partially offset by gains in the wind resource from undeveloped sites. Migration corridors are most costly when they align with the prevailing wind direction.

As offshore wind farms begin to be built along the U.S. Atlantic coast, development will most likely begin with the most upwind sites closest to the shore with a prevailing southwest wind. These wind farms will have a large impact on any further downwind farms and regulators should be mindful of this when planning and permitting initial offshore wind farms. We have shown that if the overall wind farm development is small, then a myopic planner can come very close to optimal wind farm development. However, achieving high levels of wind farm development efficiently will require an awareness of how current and future development will impact the whole of offshore wind energy development. Given the challenges provided by climate change, large scale offshore wind may be a realistic future scenario.

Funding

This work was partially supported by the NSF-sponsored IGERT: Offshore Wind Energy Engineering, Environmental Science, and Policy (Grant Number 1068864).

Acknowledgments

Our thanks to the anonymous reviewers whose thoughtful comments helped to improve the paper.

Supplementary materials

Supplementary material associated with this article can be found, in the online version, at doi:10.1016/j.ejor.2017.11.026.

References

Archer, R., Nates, G., Donovan, S., & Waterer, H. (2011). Wind turbine interference in a wind farm layout optimization mixed integer linear programming model. *Wind Engineering, 35*(2), 165–175.

Baker, E., & Solak, S. (2011). Climate change and optimal energy technology R&D policy. *European Journal of Operational Research, 213*(2), 442–454.

Barthelmie, R. J., Hansen, K., Frandsen, S. T., Rathmann, O., Schepers, J. G., Schlez, W., et al. (2009). Modelling and measuring flow and wind turbine wakes in large wind farms offshore. *Wind Energy, 12*(5), 431–444.

Berkenhagen, J., Doring, R., Fock, H. O., Kloppmann, M. H. F., Schulze, T., & Pedersen, S. A. (2010). Decision bias in marine spatial planning of offshore wind farms: Problems of singular versus cumulative assessments of economic impacts on fisheries. *Marine Policy, 34*(3), 733–736.

Drewitt, A. L., & Langston, R. H. W. (2006). Assessing the impacts of wind farms on birds. *IBIS, 148*(1), 29–42.

Elkinton, C., Manwell, J., & McGowan, J. (2008). Algorithms for offshore wind farm layout optimization. *Wind Engineering, 32*(1), 67–84.

Fischetti, M., & Monaci, M. (2016). Proximity search heuristics for wind farm optimal layout. *Journal of Heuristics, 22*(4), 459–474.

Gaumond, M., Réthoré, P.-E., Ott, S., Peña, A., Bechmann, A., & Hansen, K. S. (2014). Evaluation of the wind direction uncertainty and its impact on wake modeling at the Horns Rev offshore wind farm. *Wind Energy, 17*(8), 1169–1178.

González, J. S., Payán, M. B., Santos, J. M. R., & González-Longatt, F. (2014). A review and recent developments in the optimal wind-turbine micro-siting problem. *Renewable and Sustainable Energy Reviews, 30*, 133–144.

Hüppop, O., Dierschke, J., Exo, K. M., Fredrich, E., & Hill, R. (2006). Bird migration studies and potential collision risk with offshore wind turbines. *IBIS, 148*(1), 90–109.

Jimeńez, P. A., Navarro, J., Palomares, A. M., & Dudhia, J. (2015). Mesoscale modeling of offshore wind turbine wakes at the wind farm resolving scale: A composite-based analysis with the weather research and forecasting model over Horns Rev. *Wind Energy, 18*(3), 559–566.

Jonkman, J., Butterfield, S., Musial, W., & Scott, G. (2009). *Definition of a 5-MW reference wind turbine for offshore system development*. Golden, CO: National Renewable Energy Laboratory.

Lackner, M., & Elkinton, C. (2007). An analytical framework for offshore wind farm layout optimization. *Wind Engineering, 31*(1), 17–31.

Le Cadre, H., Papavasiliou, A., & Smeers, Y. (2015). Wind farm portfolio optimization under network capacity constraints. *European Journal of Operational Research, 247*(2), 560–574.

Liesiö, J., Mild, P., & Salo, A. (2008). Robust portfolio modeling with incomplete cost information and project interdependencies. *European Journal of Operational Research, 190*(3), 679–695.

Liesiö, J., & Salo, A. (2012). Scenario-based portfolio selection of investment projects with incomplete probability and utility information. *European Journal of Operational Research, 217*(1), 162–172.

Manwell, J. F., McGowan, J. G., & Rogers, A. L. (2009). *Wind energy explained: Theory, design and application*. Chichester, UK: Wiley.

Markowitz, H. (1952). Portfolio selection. *The Journal of Finance, 7*(1), 77–91.

National Data Buoy Center. (2015). "Station 44005 (LLNR 820) – Gulf of Maine – 78 NM East of Portsmouth, NH." National Oceanic and Atmospheric Administration (NOAA). Retrieved from http://www.ndbc.noaa.gov/station_history.php?station=44005 Accessed 21.09.15.

Peña, A., Réthoré, P. E., & Rathmann, O. (2014). Modeling large offshore wind farms under different atmospheric stability regimes with the Park wake model. *Renewable Energy, 70*, 164–171.

Salo, A., Keisler, J., & Morton, A. (2011). *Portfolio decision analysis: Improved methods for resource allocation*. New York: Springer.

Schwartz, M. N., Heimiller, D., Haymes, S., & Musial, W. (2010). *Assessment of offshore wind energy resources for the United States*. Golden, CO: National Renewable Energy Laboratory.

Sheridan, B., Baker, S. D., Pearre, N. S., Firestone, J., & Kempton, W. (2012). Calculating the offshore wind power resource: Robust assessment methods applied to the U.S. Atlantic coast. *Renewable Energy, 43*, 224–233.

Singh, K., Baker, E. D., & Lackner, M. A. (2015). Curtailing wind turbine operations to reduce avian mortality. *Renewable Energy, 78*, 351–356.

Turner, S. D. O., Romero, D. A., Zhang, P. Y., Amon, C. H., & Chan, T. C. Y. (2014). A new mathematical programming approach to optimize wind farm layouts. *Renewable Energy, 63*(10), 674–680.

U.S. Department of Energy. (2014). *Wind vision: Updating the DOE 20% wind energy by 2030 report*. Washington, D.C.: U.S. Departemnt of Energy.

U.S. Energy Information Administration (2013). *Updated Capital Cost Estimates for Utility Scale Electricity Generating Plants*. Washington, D.C.: U.S. Dept. of Energy. Retrieved from http://www.eia.gov/forecasts/capitalcost/pdf/updated_capcost.pdf.

Veeramachaneni, K., Wagner, M., O'Reilly, U.-M., & Neumann, F. (2012). Optimizing energy output and layout costs for large wind farms using particle swarm optimization. In *Proceedings of the 2012 IEEE congress on evolutionary computation (CEC)* (pp. 1–7).

Volker, P. J. H., Hahmann, A. N., Badger, J., & Jorgensen, H. E. (2017). Prospects for generating electricity by large onshore and offshore wind farms. *Environmental Research Letters, 12*, 034022.

Walker, K., Gribben, B., Adams, N., Gellatly, B., Nygaard, N. G., Marchante, J. M., et al. (2016). An evaluation of the predictive accuracy of wake effects models for offshore wind farms. *Wind Energy, 19*(5), 979–996.

Wan, C., Wang, J., Yang, G., Gu, H., & Zhang, X. (2012). Wind farm micro-siting by Gaussian particle swarm optimization with local search strategy. *Renewable Energy, 48*, 276–286.

Zhang, P. Y., Romero, D. A., Beck, J. C., & Amon, C. H. (2014). Solving wind farm layout optimization with mixed integer programs and constraint programs. *Euro Journal on Computational Optimization, 2*(3), 195–219.